23rd ABCM International Congress of Mechanical Engineering
December 6-11, 2015, Rio de Janeiro, RJ, Brazil

ANALYSIS OF TUBE-FIN 'NO-FROST' EVAPORATORS USING A DISTRIBUTED MODEL

Paulo Henrique Neves Pimenta
Department of Mechanical Engineering
Rio Verde University– UniRV, Fazenda Fontes do Saber, CEP. 75901-970 – Rio Verde, GO – Brazil
Telephone: 55 64 9291 1772 - e-mail: paulohenrique@unirv.edu.br

André Luiz Seixlack
Department of Mechanical Engineering
São Paulo State University – UNESP, CEP. 15385-000 - Ilha Solteira, SP – Brazil
Telephone: 55 18 3742 1043 - e-mail: andre@dem.feis.unesp.br

Abstract. *This work presents a numerical model to simulate the flow and heat transfer between the refrigerant fluid and outside air along tube-fin evaporators commonly used in 'no-frost' household refrigerators. The refrigerant flow inside the tube is taken as one-dimensional and divided in a two-phase flow region and a superheated vapor flow region. The homogeneous flow model is employed for the two-phase flow region. The refrigerant pressure drop and the moisture condensation on the airflow crossing the outside of the tubes are taken into account. The fundamental equations of mass conservation, momentum and energy conservation governing the refrigerant flow are solved in order to evaluate the velocity, pressure and specific enthalpy of the refrigerant fluid, respectively. The energy and mass (humidity) conservation equations for the air flow are solved in order to evaluate the temperature and absolute humidity of the air crossing the evaporator, respectively. The energy conservation equation for the wall of the evaporator tube is also solved to obtain the wall temperature distribution. The governing equations are integrated numerically using Euler's method and the resulting algebraic system of equations is solved by Newton-Raphson's method. The results are compared with experimental data available in the literature and the mean relative deviation is 1.44 % for the refrigeration capacity and mean absolute deviation is 1.02 °C for the degree of superheat at the evaporator outlet.*

Keywords: *Tube fin evaporator, Household refrigerator, 'No frost', Two-phase flow, Distributed model.*

1. INTRODUCTION

Global energy consumption is one of the most crucial current environmental issues. According to Piucco, Melo and Boeng (2005), high energy consumption is directly associated to low energy-efficient thermal systems in operation, such as domestic refrigerators, which though individually exhibit low energy consumption, the large number of appliances in operation and their low thermodynamic efficiencies make them a major contributor to the planet's energy consumption.

The top selling refrigerator models in Brazil are those that have two refrigerated compartments and automatic defrost, also known as 'no-frost' refrigerator. The main feature of these devices is the use of an air distribution system which is basically constituted of a fan, ducts and a tube-fin heat exchanger. Air aspirated by the fan passes through the evaporator where it is cooled and dehumidified. From the evaporator, the cold air is insufflated in a plenum, to provide better airflow uniformity, and part of the flow is further directed to the freezer (~ 70%) while another part is directed for the refrigerator compartment (~ 30%) (Piucco, Melo and Boeng (2005).

In the refrigeration field, an issue that has motivated intense research and substantial investment regards improving the performance of the main components of a vapor compression refrigeration system: evaporator, condenser, compressor and expansion device. The performance of these components is directly associated to the thermodynamic irreversibility resulting from the flow of the refrigerant and heat transfer process through these components, particularly in the evaporator.

The main motivation of this work is to analyze the performance of one component of a household refrigerator, the tube-fin 'no-frost' evaporator (see Fig. 1), by means of a distributed model. Several theoretical and experimental studies dealing with different aspects regarding the performance of tube-fin evaporators can be found in the literature:, Liang *et al.* (1999), Domanski, Yashar and Kim (2005), Piucco, Melo and Boeng (2005), Jabardo, Zoghbi Filho and Salamanca (2006), Byun, Lee and Choi (2007), Singh, Aute and Radermarcher (2009), Knabben, Hermes and Melo (2011), Ding *et al.* (2011), Waltrich *et al.* (2011) and Kaern, Elmegaard and Larsen (2013).

Most of the research conducted refers to heat exchangers used in commercial refrigeration and in air-conditioning systems. Due to the large amount of phenomena involved in the operation of evaporators, different aspects have been analyzed, such as how air distribution affects the evaporator performance; how shape and layout influence evaporator tubes; fin type; evaporator dynamical behavior when submitted to different operating conditions; and other aspects.

This work presents a numerical model to simulate the flow and heat transfer between the refrigerant fluid and outside air along the tube-fin evaporators commonly used in 'no-frost' household refrigerators, considering the interaction between the different tube circuit configurations. The model includes a numerical procedure that allows calculating the refrigerant mass flow rate, once the evaporator geometrical parameters and operating conditions are known, to analyze the evaporator performance. The minimization method of Levenberg-Marquardt is used to estimate the mass flow rate. The developed model is validated through a comparison with numerical and experimental data available in the literature.

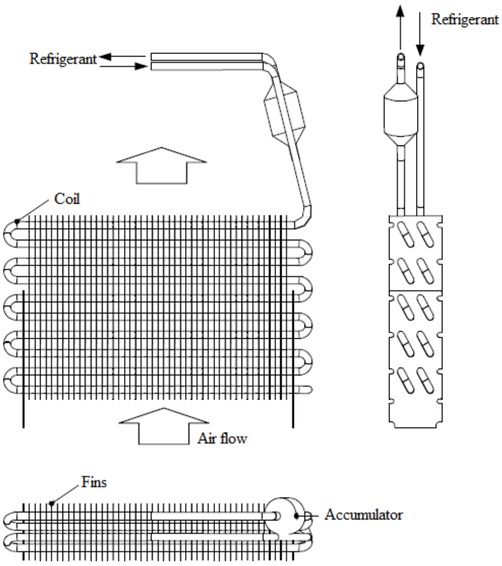

Figure 1. Tube-fin 'no-frost' evaporator (Hermes, 2006).

2. PROBLEM FORMULATION

The refrigerant fluid flow inside the evaporator tube is divided into two regions: a two-phase flow (liquid-vapor) and another one with superheated vapor flow. The pressure drop inside the tubes, due to friction and acceleration effects of the refrigerant, and the moisture condensation on the air side are taken into consideration.

The following assumptions are considered to simplify the problem: a) the refrigerant and air flow are taken to be one-dimensional; b) the refrigerant is considered as a Newtonian fluid, oil free; c) the following are disregarded: the heat conduction in the tube wall and in the axial direction of the fluid flow, the viscous energy dissipation, the potential and kinetic energy variation in the flow along the evaporator tube and the flow pulsation, refrigerator characteristic operating with positive displacement machines; d) the heat transfer coefficient is uniform on the air side may be different at dry and wet coil regions; e) there is not ice formation; f) the air flow is considered incompressible; g) the thermo-physical properties of the material of the tube wall and fins are assumed to be constant; h) the two-phase flow inside the tube is considered homogenous, i.e., the flow is mathematically treated as a pseudo single-phase flow, whose properties are obtained considering the vapor quality and properties of each individual phase. Consequently, both phases have the same velocities, pressures and temperatures and surface tension effects are not considered in any cross-section along the tube.

The governing equations for the flow inside the tube are divided according to the flow type: single-phase or two-phase. The equations presented below are related to the two-phase flow region. Considering the void fraction α = 1, in these equations the governing equations for the superheated vapor region are obtained.

Based on the above assumptions and applying the principles of mass conservation, momentum and energy conservation for the refrigerant (see Fig. 2), the following governing equations are obtained for the refrigerant flow:

$$\frac{\partial \rho}{\partial t} + \frac{\partial (\rho u)}{\partial z} = 0 \tag{1}$$

$$\frac{\partial (\rho u)}{\partial t} + \frac{\partial (\rho u^2)}{\partial z} = -\frac{\partial p}{\partial z} - F_z \tag{2}$$

$$\frac{\partial (\rho i_r)}{\partial t} + \frac{\partial (\rho u i_r)}{\partial z} = \frac{\partial p}{\partial t} + \frac{P_i}{A_{tub}} q''_{wr} \tag{3}$$

where t is the time [s], z is the coordinate along the evaporator tube [m], u is the average velocity of the refrigerant flow in the cross section of the tube [m/s], $\rho = [\alpha\rho_v + (1-\alpha)\rho_l]$ is the density of the liquid-vapor mixture [kg/m^3], $\alpha = \{1+[\rho_v(1-x)/\rho_l x]\}^{-1}$ is the void fraction, x is the vapor quality, p is the flow pressure inside the tube [Pa]. The subscripts l and v indicate the liquid and vapor phases, respectively. In equation (2), F_z is the force per volume unit due to friction between the refrigerant and the tube wall [N/m3]. This term is frequently represented by $F_z = (\partial p/\partial z)_F$, since it represents the portion of the total pressure loss along the volume control, caused by viscous effects. Thus, $F_z = (f\rho u^2/2d_i)$, in which f is the Darcy friction factor and d_i is the inner tube diameter [m].

In Equation (3), $i_r = [xi_v + (1-x)i_l]$ is the refrigerant specific enthalpy [J/kg], i_l and i_v are, respectively, the liquid and vapor specific enthalpy [J/kg], $q''_{wr} = [h_r(T_w - T_r)]$ is the heat flux from the tube wall to the refrigerant [W/m^2], h_r is the convection heat transfer coefficient inside the tube [W/m^{2}K], T_w and T_r are, respectively, the tube wall and the refrigerant temperatures [°C], $P_i = (\pi d_i)$ is the inner perimeter of the tube [m], d_i is the inner diameter of the tube and $A_{tub} = (\pi {d_i}^2/4)$ is the cross sectional area of the tube [m^2].

Appling the principle of energy conservation at the tube wall, we have,

$$m_{wf}\, c_{p,wf}\, \frac{dT_w}{dt} = h_a A'_t dz(T_a - T_w) + h_m A'_t dz\, \lambda_{water}(\omega_a - \omega_{a,sat}) - h_r P_i dz(T_w - T_r) \tag{4}$$

where m_{wf} is the mass of the tube wall and the fins by unity length [kg/m], $c_{p,wf}$ is the mean specific heat at constant pressure considering the tube and fin materials [J/kg K], h_a is the air side convection heat transfer coefficient [W/m^2 K], $A'_t = (A'_r + A'_f \eta_f)$ is the heat transfer total area per unit length [m], A'_r is the outer area not covered by fins per unit length [m], A'_f is the fin surface area per unit length [m], η_f is the fin efficiency presented by McQuiston and Parker (1994), T_a is the air temperature [°C], λ_{water} is the latent heat of water condensation at temperature T_w [J/kg], ω_a and $\omega_{a,sat}$ are the air absolute humidity and the saturated air humidity at temperature T_w [kg$_v$/kg$_{dry\ air}$], respectively, and h_m is the mass transfer coefficient [kg/m^{2}s], calculated by the Lewis correlation, $[h_m = h_a/Le\ c_{p,a}]$, where Le is the Lewis number, $L_e = [k_a/(\rho_a c_{p,a} D_{ab})]$, D_{ab} is the water-air mass diffusivity [m^2/s], k_a is the air thermal conductivity [W/mK] and $c_{p,a}$ is the specific heat at constant pressure for the air [J/kgK].

In tube-fin evaporators used in conventional refrigeration systems, the occurrence of air dehumidification is common. The air-side surface of the coil will be covered by a liquid water film because of dehumidification, which may freeze due to low evaporating temperatures. Thus, in addition to sensible heat transfer resulting from the temperature variation, there is the latent heat transfer due to the condensation. To obtain the governing equations for the air flow, in addition to the previous assumptions, the thermal inertia of the air is neglected.

Applying the principles of mass conservation (humidity) and energy conservation for the air (Kuehn, Ramsey and Threlkeld, 1998), the following equations are obtained, respectively,

$$\dot{m}_a \frac{d\omega_a}{dy} dy = h_m A'_t dz(\omega_a - \omega_{a,sat}) \tag{5}$$

$$\dot{m}_a \frac{di_a}{dy} dy = h_a A'_t dz(T_a - T_w) + h_m A'_t dz\, \lambda_{water}(\omega_a - \omega_{a,sat}) + h_m A'_t dz(\omega_a - \omega_{a,sat}) i_{l,water} \tag{6}$$

where $\dot{m}_a = [\rho_a u_a (W_{evap} L_{evap})]$ is the air mass flow rate [kg/s], y is the coordinate along the airflow crossing the outside of the evaporator tube [m], ρ_a is the air density [kg/m^3], u_a is the air velocity [m/s], L_{evap} and W_{avap} are the straight length and width of evaporator [m], $i_{l,water}$ is the liquid water specific enthalpy at temperature T_w [J/kg].

Thus, the proposed model is constituted by the system of Eqs. (1) to (6), which should be solved to give the distributions of u, p, i_r, T_w, ω_a and T_a, respectively. To perform this task, closer relationships are then needed to calculate the refrigerant, air and water thermo-physical properties, the friction coefficient, the refrigerant-air heat transfer coefficients and the water mass-transfer coefficient.

The refrigerant and air thermo-physical properties are obtained, respectively, from REFPROP 8.0 (Lemmon, Huber and McLinden, 2007) and from the data presented by ASHRAE (1993). The thermo-physical properties of water, of the tube wall and fin materials are computed using the data provided by Incropera, *et al*. (2014). Moreover, the model uses the following correlations to compute other parameters:

1. friction factor in the superheated vapor region: Churchill (1977);
2. pressure drop due to friction in the two-phase flow region: Paliwoda (1989);

3. heat transfer coefficient in the single-phase flow region: Dittus-Boelter (1930);
4. heat transfer coefficient in the two-phase flow region: Jung and Radermacher (1991);
5. heat transfer coefficient on the air side: McQuiston (1981).

2.1 Initial conditions

For a given tube-fin evaporator the model could be used to: (a) determine evaporator performance parameters, such as: refrigeration load; outlet refrigerant and air temperatures; among others, since the evaporator operating conditions and dimensions are known. In this case a direct problem is solved from a set of inlet conditions for the refrigerant and also for the air; (b) determine the refrigerant mass flow rate along evaporator tubes, once its dimensions and other operating conditions are known. In this case, an inverse problem must be solved, since the governing equations are mass flow rate dependent. The initial conditions for each case is shown as follows.

(a) Direct problem: in this case, the solution of Equations (1) to (6) is obtained from known refrigerant conditions at the tube inlet *(z=0)*: $\dot{m}_r$, x, p and T_r, and from known air conditions T_a, ω_a and $\dot{m}_a$ at evaporator inlet. Knowing x and T_r at the tube inlet, the other thermodynamic properties are calculated at this point: $\rho=\rho(T_r, x)$ and $i_r=i_r(T_r, x)$, using the thermodynamic library REFPROP 8.0 (Lemmon, McLinden and Huber, 2007). The tube wall temperature is assumed equal to the refrigerant temperature at z=0 and the air specific enthalpy, also at z=0, is obtained as a function of T_a and ω_a, $i_a=i_a(T_a, \omega_a)$, from the data presented by ASHRAE (1993). The density and temperature of the refrigerant in the two-phase and single-phase regions are also obtained by thermodynamic library REFPROP 8.0, using the pressure values, the specific refrigerant enthalpy and vapor quality, at single phase region by: $\rho = \rho(p, i_r)$ and $T_r = T_r(p, i_r)$ and at two-phase region by: $\rho = \rho(p, x)$ and $T_r = T_r(p)$.

(b) Inverse problem: The inverse problem corresponds to that which is needed to calculate the refrigerant mass rate along the evaporator once its geometry is known and the other refrigerant conditions at the tube inlet: x, p and T_r, and from known air conditions T_a, ω_a and $\dot{m}_a$ at evaporator inlet. The problem is non-linear because the governing equations are mass dependent.

3. SOLUTION METHODOLOGY

The numerical solution for the system of Equations (1) to (6) is obtained by numerical integration using the Euler method, in which the Equations (1) to (3) are integrated over time and space, z direction, between the points k-1 and k along the tube (see Fig. 2), Equation (4) is time integrated and the Equations (5) and (6) are integrated in the y direction. Unsteady terms in governing equations are discretized using the approximation formula: $\partial\varphi / \partial t = [(\varphi - \varphi^o) / \Delta t]$, in which superscript "o" means the time step immediately before. For the integrals over time a completely implicit scheme was used, in order to reach numerical stability for the algorithm.

The evaporator is divided in small cells, a total of Mk cells, with same dimensions Δz, as shown in Figures 2 and 3. The discretized equations for calculating the variables present the same form for all points. To avoid the use of a separate equation for the point k=1, the evaporator inlet, a dummy cell is used in this position. Variables u, p, i_r and T_w are stored at the k-1 and k points of the cell, shown in Figure 2, while the variables T_a and ω_a are stored on the *(i,j)*, *(i,j+1)*, *(i+1,j)* and *(i+1,j+1)* points of the cell, also shown in Figure 2.

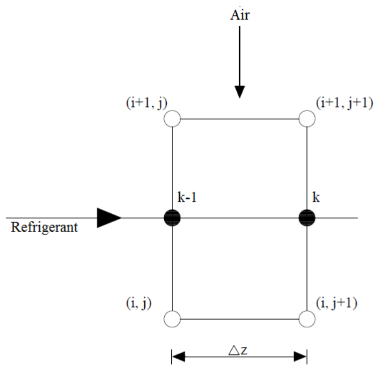

Figure 2. Layout of the limits of integration along the refrigerant fluid flow and air flow.

The solution of the resulting algebraic system of equations is obtained for each cell along the evaporator and the variables u ,p, i_r, T_w, ω_a and T_a are calculated at every point. To improve the efficiency of the solution process, a two-level iterative method is used. First, the refrigerant and tube wall variables are calculated. Second, the air variables are calculated. The Newton-Raphson method is applied point by point along the evaporator to solve the system of equations.

In the airside, the temperature and humidity values are corrected for the whole mesh and not cell by cell. Convergence is achieved when the summation of all corrections of the air conditions, T_a and ω_a, will be less than 10^{-4}. It is considered that steady state regime is reached when a change of u, p, i_r and T_w, from a time step to another is less than 10^{-3}. Once the steady state regime is achieved, the refrigerant mass flow rate is increased or decreased to simulate the evaporator unsteady behavior. As the evaporator was in steady state regime, this perturbation will promote an unsteady state period followed by a steady state. This change in refrigerant mass flow rate simulates different operating system conditions.

For the grid shown in Fig. 3 *NR* index relates to the line, *ii* refers to the vertical position of the tubes and *jj* refers to a horizontal position along the tubes.

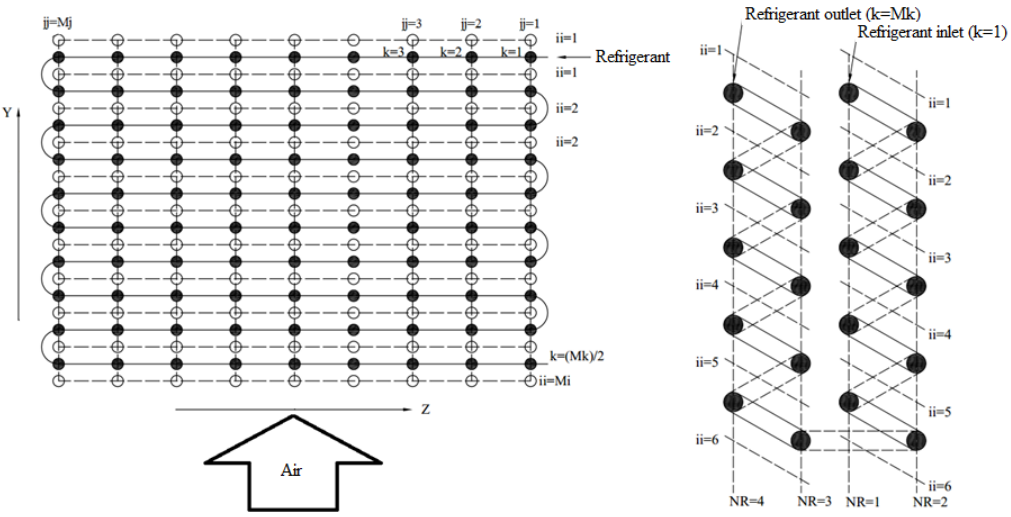

(a) (b)

Figure 3. Discretization of the evaporator for the numerical solution: (a) front view; (b) lateral view.

Since the inverse problem is non-linear as the governing equations are mass dependent, an additional calculation procedure is necessary. Therefore, the initial value of $\dot{m}_r$ is estimated and the refrigerant temperature at the evaporator outlet ($T_{r,o}$) is calculated and compared to the respective measured (or computed using another model) value. After, the value of $\dot{m}_r$ is corrected by using the non-linear parameter estimation method of Levenberg-Marquardt. The process is repeated until some convergence criteria are matched.

4. RESULTS AND DISCUSSION

This work presents some comparison between results for the steady state regime computed using the present model and results obtained by Liang *et al*. (1999), for the direct problem. Table 1 shows the geometrical parameters for the evaporator analyzed by Liang *et al.* (1999).

Table 1. Geometrical parameters of the evaporator simulated by Liang *et al*. (1999).

Geometrical parameters			
Straight tube length (m)	1.0	Tube inner diameter (mm)	8.83
Transversal tube spacing (m)	0.025	Fins thickness (mm)	0.12
Longitudinal tube spacing (m)	0.0216	Fins spacing (mm)	2.41
Tube outer diameter (mm)	9.53	Quantity of fins	394

Figures 4(a) and 4(b) show, respectively, the relative humidity of air at evaporator inlet, R.H., of 30% and 60%, some comparisons of the air temperature profile, the tube wall temperature and the refrigerant temperature calculated using the present model with the results computed by Liang *et al*. (1999). For these cases, the direct problem is solved considering known refrigerant mass flow rate of 12.96 kg/h and 30.96 kg/h and the refrigerant temperature at the tube inlet of 10.5 °C and 11 °C, for the air relative humidity at the evaporator inlet of 30 % and 90 %, respectively. The other operating conditions used by Liang *et al.* (1999) were kept constant for such cases: vapor quality at tube inlet = 0.22, air temperature and air velocity at the evaporator inlet are 28 °C and 2.0 m/s, respectively. The enthalpy at evaporator inlet is determined through operating conditions at the condenser outlet: condensation temperature = 45°C, sub-cooling degree = 5°C.

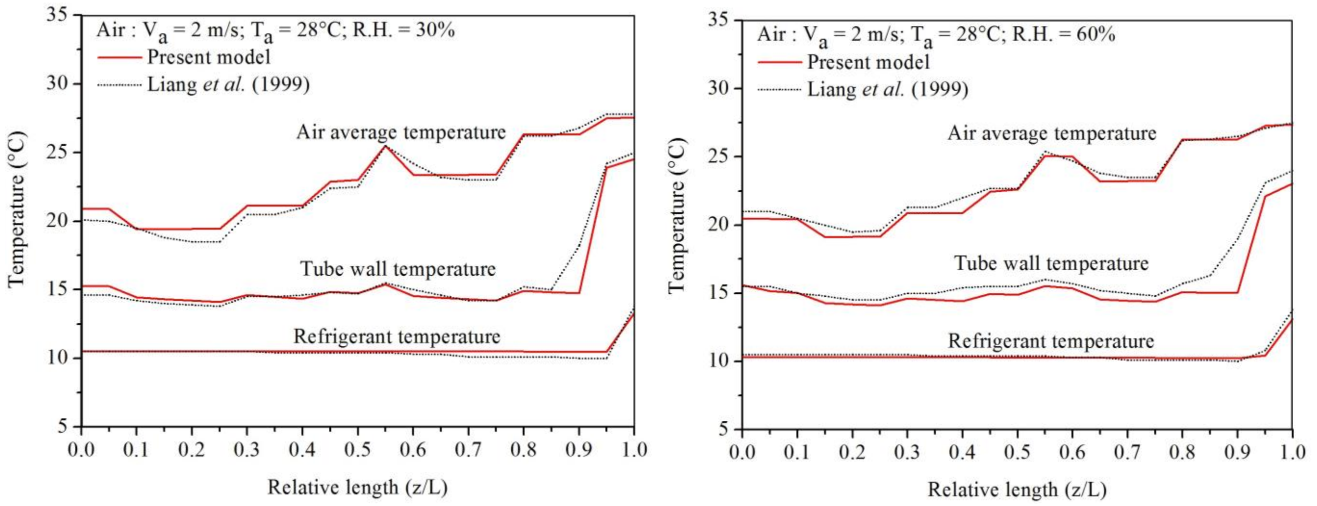

(a) (b)

Figure 4. Temperature profiles for air, tube wall and refrigerant for: (a) R.H. = 30%; (b) R.H. = 60%.

Figures 4(a) and 4(b) show a good agreement between the results presented by Liang *et al.* (1999) and the results calculated using the present model, mainly for refrigerant and tube wall temperature profiles. However, the air temperature profile still has discontinuities that need further investigation. Note that the refrigerant and the tube wall temperatures suddenly increase near the tube outlet due to the complete vaporization of the refrigerant in this region. As observed by Liang *et al.* (1999), the higher air relative humidity at the evaporator inlet results in higher total air heat transfer coefficient due to the intensification of mass transfer along the coil, caused by increased moisture condensation. Due to this, the increased air relative humidity at the evaporator inlet causes the tube wall temperature to increase, as shown in Figures 4 (a) and 4 (b).

The results obtained from the model for steady state regime were also compared to the experimental data obtained by Piucco, Melo and Boeng (2005). These comparisons refer to the set of tests in which only the refrigerant mass flow rate and the 3 were different, as shown in Table 2. The other operating conditions were kept constant: refrigerant temperature at the tube inlet of -33 °C, evaporation pressure 0.73 bar, vapor quality at tube inlet 0.42 and air volumetric flow rate 38 m^3/h. The geometrical parameters for the evaporator tested are presented in Table 3.

Table 2. Operating conditions (Piucco, Melo and Boeng, 2005).

	Tests					
	1	2	3	4	5	6
Refrigerant mass flow rate (kg/h)	2.62	2.98	3.22	3.48	3.52	3.6
Air temperature at the evaporator inlet (°C)	-12.5	-17.6	-20.5	-20.8	-20.8	-21

Figures 5(a) and 5(b) show, respectively, the cooling capacity as a function of refrigerant mass flow rate and the evaporator superheat as a function of refrigerant mass flow rate. The calculated values are compared with experimental data provided by Piucco, Melo and Boeng (2005) in Figures 5(a) and 5(b). The evaporator superheat is the refrigerant superheat degree at the evaporator outlet (ΔTo), which is calculated from the difference between the refrigerant temperature at the outlet of the evaporator (Tr,o) and the evaporation temperature ($Tsat$): $\Delta T_o = T_{r,o} - T_{sat}$.

Table 3. Geometrical parameters of the evaporator tested by Piucco, Melo and Boeng (2005).

Geometrical parameters			
Number of tube rows	4	Tube outer diameter (mm)	7.94
Tube number in each row	5	Tube inner diameter (mm)	6.97
Total length of the coil (m)	7.814	Fins spacing (mm)	6.35
Number of vertical tube pitch	10	Fins thickness (mm)	0.15
Number of horizontal tube pitch	2	Fin type	Lisa
Vertical tube spacing (mm)	19.2	Number of fins	47
Horizontal tube spacing (mm)	11.1	Face area, m²:	0.02083

It can be seen in Figure 5(a) that the computed results follow the same trend and show good agreement with the experimental data. Furthermore, all the calculated values for the cooling capacity were higher than the experimental data. Considering the entire range of mass flow rate analyzed, 2.62 to 3.6 kg/h, the mean relative deviation and the mean absolute deviation, compared to the experimental data of Piucco, Melo and Boeng (2005), are 1.44% or 1.63 W, respectively.

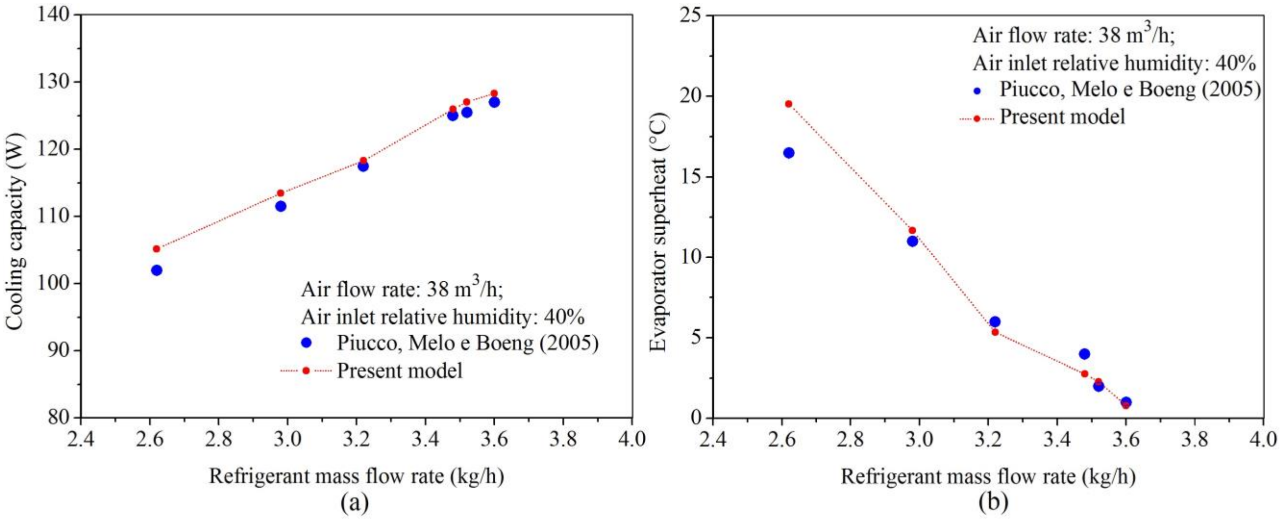

Figure 5. Comparisons between computed values and experimental data (Piucco, Melo and Boeng, 2005): (a) cooling capacity as a function of refrigerant mass flow rate; (b) refrigerant superheat degree as a function of refrigerant mass flow rate.

Figure 5(b) shows that the computed results also follow the same trend and show good agreement with the experimental data. It was also noted that the model overestimates the evaporator superheat over the range of flow mass rate up to 3.0 kg/h. The largest deviation occurred for the mass flow rate of 2.62 kg/h, where the absolute deviation between the computed and experimental evaporator superheat was 3.03 °C. This behavior, as shown by Piucco, Melo and Boeng (2005), is due to the difficulty in measuring superheat degrees less than 2 °C due to the presence of liquid in suspension in the flow, which decreases the measurement accuracy of the superheat degree. Taking into account the entire range of mass flow rate analyzed, 2.62 to 3.6 kg/s, the mean absolute deviation is 1.02 °C, compared to the experimental data of Piucco, Melo and Boeng (2005).

Figure 6 shows the comparison between computed cooling capacity as a function of evaporator superheat and the experimental data provided by Piucco, Melo and Boeng (2005). Figure 6 shows that the cooling capacity is inversely proportional to the evaporator superheat, since a lower degree of overheating means a greater extension of the two-phase region, which results in a greater cooling capacity.

Moreover, Figure 4 (a) indicates that the cooling capacity is directly proportional to mass flow rate. The model's tendency to overestimate the cooling capacity is also observed.

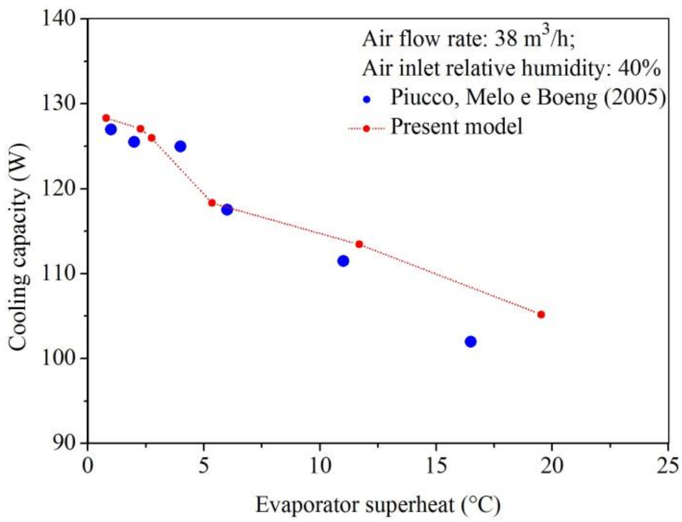

Figure 6. Comparison between computed values and experimental data (Piucco, Melo and Boeng, 2005) of the cooling capacity as a function of evaporator superheat.

5. CONCLUSION

This work presents a model for analyzing the tube-fin evaporator, commonly used in refrigeration and air conditioning systems. In the distributed model the refrigerant flow inside the tubes and the heat transfer to the outside air are considered. The refrigerant flow is divided into two regions: a vapor-liquid two-phase flow and a flow of superheated steam. The refrigerant pressure drop, the moisture condensation on the airflow crossing the outside of the tubes and the interaction between the different circuit configurations of the tubes are also taken into account.

The model allows calculating, in steady-state and unsteady operations, the cooling capacity, the evaporator superheat, the refrigerant mass flow rate, the local distribution of refrigerant and air temperatures, the refrigerant velocity, the refrigerant pressure and the air humidity, known geometrical parameters of the evaporator and other operating conditions.

Comparison between experimental results available in open literature and those obtained in this work show good agreement with regard to the refrigerant mass flow rate, as well as evaporator superheat. Considering the entire range of mass flow rate analyzed, 2.62 to 3.6 kg/h, the mean absolute deviation in relation to the experimental data, regarding the refrigerant mass flow rate and the evaporator superheated, was 1.02 °C, and the mean relative deviation in relation to the experimental data, regarding the refrigerant mass flow rate and the cooling capacity, was 1.44 %.

The Euler method used to integrate the equations and the Newton-Raphson method used to solve point by point the system of discretized equations proved to be very reliable to solve the governing equations of the system.

6. REFERENCES

ASHRAE, 1993. *Fundamental Handbook*, American Society of Heating, Refrigerating and Air-Conditioning Engineers, chapter 06.

Byun, J., Lee, J. and Choi, J., 2007. "Numerical analysis of evaporation performance in a finned-tube heat exchanger". *International Journal of Refrigeration*, v.30, p. 812-820.

Churchill, S. W., 1977. "Friction factor equation spans all fluid flow regimes". *Chemical Engineering*, v. 84, p. 91-92.

Ding, W.K., Fan, J.F., He, Y.L., Tao, W.Q., Zheng, Y.X., Gao, Y.F. and Song, J.., 2011, "A general simulation model for performance prediction of plate fin-and-tube heat exchanger with complex circuit configuration". *Applied Thermal Engineering*, v.31, p. 3106-3116.

Dittus, F., and Boelter, L., 1930. "Heat transfer in automobile radiators of the tubular type". *University of California Publications in Enginnering*, v.12, p. 443-461.

Domanski, P.A., Yashar, D., Kim, M., 2005. "Performance of a finned-tube evaporator optimized for different refrigerants and its effect on system efficiency". *International Journal of Refrigeration*, London, v.28, p. 820-827.

Incropera, F.P., Dewitt, D.P, Bergman, T.L, Lavine, A.S., 2014, *Fundamentos de Transferência de Calor and Massa*, Editora: LTC, ISBN 8521625049, 7ª. Ed., Rio de Janeiro, 650 p.

Jabardo, J. M. S.; Zoghbi Filho, J. R. B.; Salamanca, A., 2006. "Experimental study of the air side performance of louver and wave fin-and-tube coils". *Experimental Thermal and Fluid Science*, v. 30, p. 621-631.

Kaern, M.R., Elmegaard, B. and Larsen, L.F., 2013. "Comparison of fin-and-tube interlaced and face split evaporators with flow maldistribution and compensation". *International Journal of Refrigeration*, v.36, p. 203-214.

Knabben, F.T., Hermes, C.J. and Melo, C., 2011, "In-situ study of frosting and defrosting processes in tube-fin evaporators of household refrigerating appliances". *International Journal of Refrigeration*, v.34, p. 2031-2041.

Lemmon, E. W., Huber, M. L., McLinden, M. O., 2007, *NIST Reference Fluid Thermodynamic and Transport Properties – REFPROP, Version 8.0*. NIST, Standard Reference Database 23, Gaithersburg.

Liang, S.Y., Liu, M., Wong, T.N, and Nathan, G.K., 1999, "Analytical Study of Evaporator Coil in Humid Environment", *Applied Thermal Engineering*, v. 19, pp. 1129-1145.

McQuiston, F. C., 1981. "Finned tube heat exchangers: state of the art for the air side". *ASHRAE transactions*, London, v.87, p. 1077-1085.

Paliwoda, A., 1989. "Generalized method of pressure drop and tube length calculation with boiling and condensing refrigerants within the zone of saturation". *International Journal of Refrigeration*, v.12, p. 314-322.

Piucco, R.O., Melo, C., Boeng, J., 2005. "In-situ performance evaluation of air distribution systems of no-frost refrigerators, In: *VII Congresso Iberoamericano de Ar Condicionado, Aquecimento e Refrigeração –CIAR,* **Anais,** Montevideo, Uruguai. (in Portuguese)

Singh, V., Aute, V. and Radermarcher, R.A., 2009. "A heat exchanger model for air-to-refrigerant fin-and-tube heat exchanger with arbitrary fin sheet". *International Journal of Refrigeration*, v.32, p. 1724-1735.

Waltrich, P.J., Barbosa Junior, J.R., Hermes, C.J. and Melo, C., 2011. "Air-side heat transfer and pressure drop characteristics of accelerated flow evaporators". *International Journal of Refrigeration*, v.34, p. 484-497.

7. RESPONSIBILITY NOTICE

The authors are the only responsible for the printed material included in this paper.